Effect of temperature on the gas-phase photocatalytic H₂ generation using microreactors under UVA and sunlight irradiation

Alejandra Castedo[1], Albert Casanovas[1], Inma Angurell[2], Lluís Soler[1,3*], Jordi Llorca[1,3]

[1]Institute of Energy Technologies and Barcelona Research Center in Multiscale Science and Engineering, Universitat Politècnica de Catalunya. Eduard Maristany 10-14, EEBE, 08019 Barcelona, Spain.

[2]Department of Inorganic Chemistry, Universitat de Barcelona. Martí i Franquès 1, 08028 Barcelona, Spain.

[3]Departament d'Enginyeria Química, Universitat Politècnica de Catalunya. Eduard Maristany 10-14, EEBE, 08019 Barcelona, Spain.

*Corresponding author:

Dr. Lluís Soler

Universitat Politècnica de Catalunya

Eduard Maristany 10-14, EEBE

08019 Barcelona, Spain

Tel.: (+34) 93 401 07 80

e-mail: lluis.soler.turu@upc.edu

Abstract

The effect of temperature on the photocatalytic hydrogen generation from a gaseous water-ethanol mixture has been tested in a silicone microreactor containing nine microchannels of 500 μm (width) x 1 mm (depth) x 47 mm (length) coated with Au/TiO_2 photocatalyst under UVA irradiation. Kinetic analyses have indicated that the hydrogen production rate follows the Langmuir-Hinshelwood model. The effect of temperature from 298 to 348 K has been determined by thermodynamic parameters, such as enthalpy ($\Delta H^{\neq}$), entropy ($\Delta S^{\neq}$) and Gibbs free energy ($\Delta G^{\neq}$) of activation, using the transition state theory (TST). The apparent rate constants (k_{app}) are higher by increasing the temperature, and the activation energy has been determined to be 24 ± 1 $kJ \cdot mol^{-1}$. In order to evaluate if solar concentration could be used to enhance the photoproduction of hydrogen, the reaction has also been conducted under direct sunlight using a solar concentrator of about 1 m in diameter. Finally, the microreactor has been scaled up by a factor of ca. 10 to a device containing thirty two microchannels of 500 μm (width) x 1 mm (depth) x 117.5 mm (length). The specific (i.e per irradiated area of catalyst) hydrogen production rates of both microreactors using sunlight are very similar suggesting that this technology could lead to viable solar hydrogen production.

1. Introduction

Hydrogen as a sustainable energy carrier has received much attention over the last years, becoming a promising alternative to manage renewable energy more efficiently. However, most of the hydrogen is obtained nowadays from fossil fuels, such as natural gas and petroleum fractions, mainly by steam reforming and partial oxidation processes, which lead to CO_2 emissions [1]. Among the existing renewable energy-based processes of hydrogen production, solar energy is the most versatile form of renewable energy to use water as a source of hydrogen [2]. Solar energy can be used to generate hydrogen in the form of heat (thermochemistry), photons (photochemistry or photovoltaic) or electricity (electrolysis). Among them, photocatalytic systems are potentially the most efficient to carry out water splitting for hydrogen production, so that photon energy is directly converted into chemical energy, whereas the other processes have loses associated with thermal transformations or with the conversion of solar energy to electricity [3].

Oxide semiconductors, such as TiO_2, are promising candidates for photocatalytic water splitting. The advantages of TiO_2 over other oxide semiconductors are its availability, high chemical stability, non-toxicity and low cost. Surface functionalization of TiO_2 with transition metal oxides or noble metals such as Pt, Pd, Au and Ag or bimetallic alloy nanoparticles has been found to enhance hydrogen production by facilitating electron transfer and therefore inhibiting electron-hole recombination, as well as by improving the photocatalytic response under the visible region [4–11]. On the other hand, some of the problems related to inefficient solar light responsive photocatalysts

for water splitting can be overcome by adding sacrificial agents, typically alcohols, as they increase charge-separation efficiency and give higher H_2 generation rates. Ethanol and methanol are considered excellent hole scavengers because they are readily available, easy to obtain from biomass and, concerning ethanol, safe to handle. The oxidative potentials of ethanol and methanol are 0.08 and 0.03 V, respectively, which are substantially lower than that of water (1.23 V), so they can be more easily oxidized than water by the holes in the valence band of the photoexcited semiconductor [12–15]. Up to now, most of the researches on photocatalytic hydrogen production have been focused on developing new photocatalytic materials and testing different sacrificing reagents and light intensities [16]. In contrast, there are very few works focused on the effect of temperature on the photogeneration of hydrogen. There are several studies that have revealed an interesting synergetic effect between light and heat [10,17,18]. This is particularly important since around 50% of the overall solar energy that reaches Earth's surface is derived from the infrared band of the spectrum, which is perceived as heat [19].

The manufacture of silicone microreactors for photocatalytic reactions using 3D printed molds allows a simple, cheap and reproducible fabrication method of UV-light transparent microreactors with custom-made dimensions and flexible in design [20] We have recently reported a kinetic analysis for the gas-phase photogeneration of hydrogen at room temperature in a silicone microreactor coated with Au/TiO$_2$ expressed in terms of the Langmuir-Hinshelwood (L-H) model. The apparent rate constant (k_{app}) was found to be proportional to the intrinsic kinetic rate constant (k), which depends on the light intensity (I) as

$k_{app}=k \cdot I^{0.65}$ [21]. L-H can fit many photocatalytic processes, although it does not illustrate the microscopic process of photocatalysis. In this work, we extend our work on photocatalytic hydrogen production in silicone microreactors by studying the effect of temperature under UVA. We have first found out an intrinsic relation between thermodynamics and kinetics in the photocatalytic process. For this purpose, Arrhenius theory and transition state theory (TST) have been used for the first time to describe the temperature dependence of the hydrogen photoproduction rate. Standard enthalpy ($\Delta H^{\neq}$), entropy ($\Delta S^{\neq}$), Gibbs free energy ($\Delta G^{\neq}$) and activation energy (E_a) values have been calculated. Finally, we have exploited the modularity of microreactors to demonstrate an easy and cheap scale up of the process. We have used silicone microreactors, direct sunlight and a solar concentrator to increase the efficiency of the solar driven hydrogen production.

2. Experimental section

2.1. Fabrication of microreactors

The two silicone microreactors used to carry out the photocatalytic generation of hydrogen are shown in Fig.1. One of them (Fig.1A) contains nine microchannels of 500 μm (width) x 1 mm (depth) x 47 mm (length) and two headers to facilitate gas distribution. The other (Fig.1B) is the result of scaling up by a factor of ca. 10 the irradiated area of photocatalyst. It consists of thirty two microchannels of 500 μm (width) x 1 mm (depth) x 117.5 mm (length). The fabrication of silicone microreactors by casting polydimethylsiloxane (PDMS) has been reported previously [20]. A suspension of Au/TiO$_2$ in ethanol was prepared and deposited

5

onto the walls of the microchannels by means of a 1 ml analytical microsyringe, in order to reach a photocatalyst loading of ca. 2.4 mg cm^{-2}. To achieve a proper immobilization of the photocatalyst, the microchannels were previously exposed to a corona discharge (air) plasma treatment (BD-20AC Electro-Technic Products) to produce a silanol-terminated surface. The catalyst was prepared by incipient wetness impregnation over commercial TiO$_2$ (Degussa P90) from a toluene solution containing pre-formed Au nanoparticles (3-4 nm in diameter, final metal loading of 1.8 wt. %). The preparation of the dodecanethiol-capped monometallic Au nanoparticles was detailed in ref. [11,22]. An optimum Au loading of 1-2 wt. % was reported in previous studies [4,9,10]. The photocatalyst was calcined at 673 K for 2 h (2 K·min^{-1}) to remove the dodecanethiol protecting shell around the Au nanoparticles used to prevent agglomeration and also to ensure a good contact between Au and TiO$_2$ [23]. The characterization of the Au/TiO$_2$ photocatalyst and its deposition on the microchannels has been already studied by scanning electron microscopy, X-ray diffraction, UV–vis reflectance spectroscopy, transmission electron microscopy and X-ray photoelectron spectroscopy [20,21]. This methodology allowed to obtain a homogeneous Au/TiO$_2$ layer (average thickness of ca. 8±2 µm) coating the reactor microchannels [21]. After depositing the photocatalyst onto the microchannels, the microreactor was sealed with a PDMS cover using a corona plasma treatment [20].
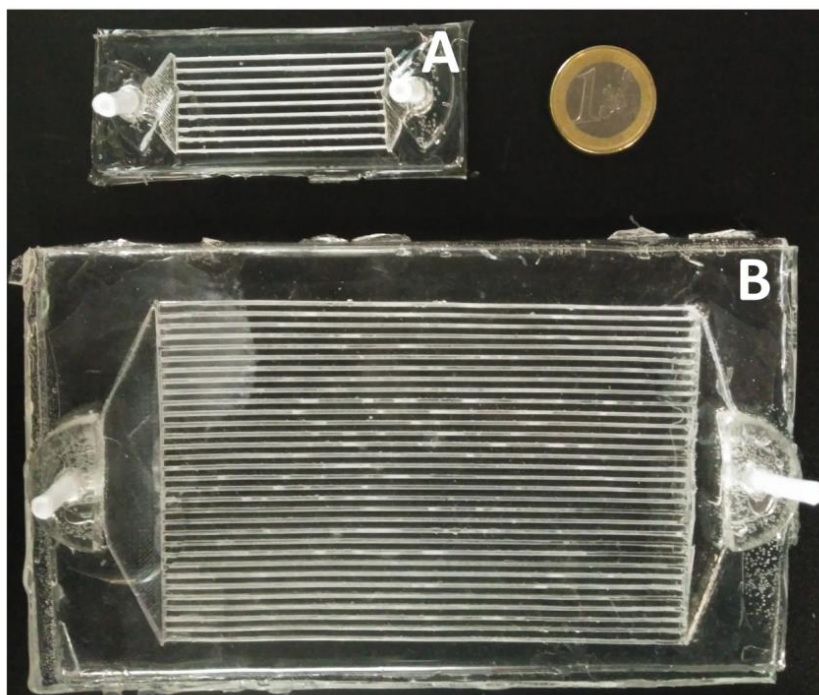
Figure 1. Photographs of the silicone microreactors used in this work. (A) microreactor with 9 microchannels of 500 µm (width) x 1 mm (depth) x 47 mm (length). (B) microreactor with 32 microchannels of 500 µm (width) x 1 mm (depth) x 117.5 mm (length). 1€ coin diameter, 23.25 mm.

2.2. Experimental setup for indoor photocatalytic H_2 production

Indoor photocatalytic tests were carried out over the microreactor shown in Fig. 1A at 298, 323, and 348 K inside an oven (Memmert UNE 200) by using two high-efficacy LEDs emitting at 365±2 nm (LED Engin LZ1-10U600) connected to an adjustable regulated DC power supply (Grelco, model G1307). The radiation intensity at the microreactor surface was varied between 0 and 23 mW·cm^{-2} for each temperature by tuning the current-voltage output of the power supply. The radiation power was measured using a UVA sensor (model PMA 2110, Solar Light Co.), which registers the UV radiation within a spectral response of 320-400 nm, connected to a radiometer (model PMA2200, Solar

Light Co.), which gives the measured irradiance in $mW \cdot cm^{-2}$. The experiments were carried out in gas phase at atmospheric pressure under dynamic conditions. The experimental setup consisted of an argon stream bubbled through a saturator containing a mixture of water:ethanol (>99.9%, Scharlau); the resulting gaseous mixture of water:ethanol (90:10, molar basis) was directly introduced into the microreactor, which was previously purged with an Ar stream, at a residence time of 0.35 s (GHSV of 10,200 h^{-1}). The effluent was monitored online every 3.5 min with an Agilent 490 Micro gas chromatograph equipped with MS 5 Å, Plot U and Stabilwax columns for a complete analysis of products. No hydrogen was generated at any temperature in dark conditions.

2.3. Experimental setup for outdoor photocatalytic H_2 production

Photocatalytic tests using direct sunlight were conducted up to 423 K over the two microreactors shown in Fig. 1 with a commercial parabolic aluminum reflector (AlSol K10, Spain). The solar reflector had a diameter of 1 m and an aperture area of 0.8 m^2 (Fig. 2). The photocataytic tests were carried out in Barcelona (Latitude 41.38°, longitude 2.17°) from June to July 2016 and from 1:00 pm to 4:00 pm GMT+2, approximately. The global solar radiation and the UVA radiation were measured with a pyranometer (Kipp & Zonen, model CM11) and a UV radiometer (Kipp & Zonen, model UVS-A-T), respectively. The measured average values for global solar radiation and UVA radiation during the mentioned periods were 90±5 $mW \cdot cm^{-2}$ and 5.0±0.5 $mW \cdot cm^{-2}$, respectively. The microreactors were placed in the collector focus, irradiating the top cover with sunlight gathered by the parabolic mirror and the bottom of the reactor with direct sunlight. The temperature was measured with five K-type thermocouples

(Fig. 2). The experimental procedure was exactly the same as the one described in section 2.2, except that the residence time was increased up to 3.2 s (GHSV of 1,130 h^{-1}) when the large microreactor (Fig. 1B) was used.
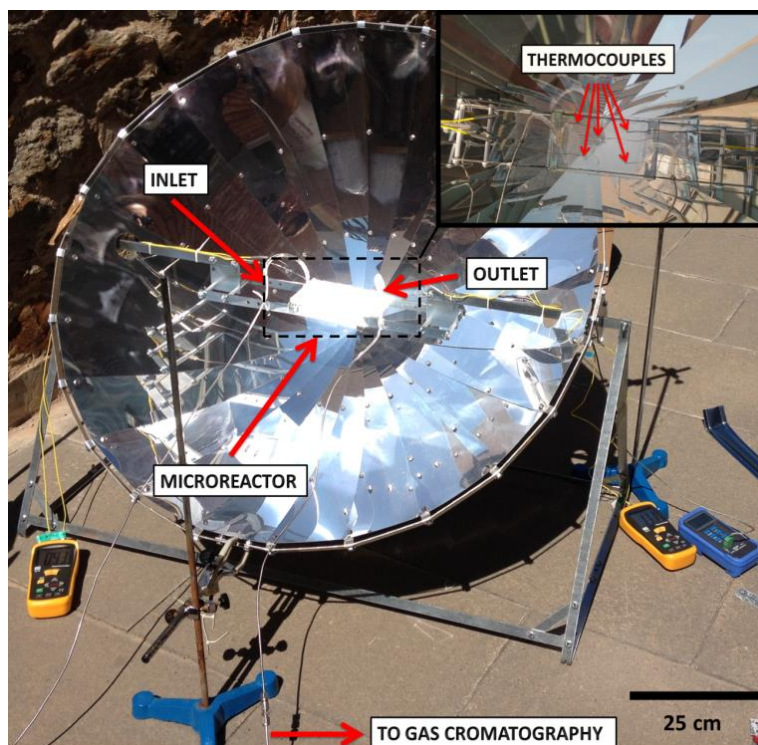

Figure 2. Photograph of the outdoor experimental test setup.

3. Analysis of kinetic and thermodynamic parameters

Recently, we have reported that the rates of hydrogen production (R_{H2}) at room temperature by using silicone microreactors loaded with Au/TiO$_2$ and using ethanol as sacrificial agent follow a Langmuir-Hinshelwood-type equation, Eq. (1). The only reaction products detected were hydrogen and acetaldehyde in a stoichiometric proportion and no other byproducts were detected, hence the overall reaction was the dehydrogenation of ethanol into acetaldehyde and hydrogen, in accordance with previous studies [6,21].

$$R_{H_2} = \frac{k_{app} \, KP_{EtOH}}{1 + KP_{EtOH}} \tag{1}$$

P_{EtOH} is the partial pressure of EtOH, K is an equilibrium pseudo constant, and k_{app} is an apparent kinetic constant that depends on the intrinsic kinetic constant k and the light intensity I as shown in Eq. (2).

$$k_{app} = k\, I^\alpha \tag{2}$$

The best fit was obtained with the following values of the kinetic parameters at room temperature: $\alpha=0.65\pm0.03$, $K=16\pm2$ kPa^{-1}, and $k=2.8\pm0.2$ µmol H_2·cm$^{1.3}$·min^{-1}·g$_{cat}^{-1}$·mW$^{-0.65}$). Taking into account that the model presented above is restricted to the macroscopic level, here we attempt to gain microscopic knowledge by understanding the effect of temperature on the photocatalytic hydrogen production. Now the k_{app} will be a function of both temperature and light intensity, so that there will be an intrinsic kinetic constant k for each temperature as shown in Eq. (3), being the apparent rate constant expressed by the Arrhenius relation (Eq. (4)),
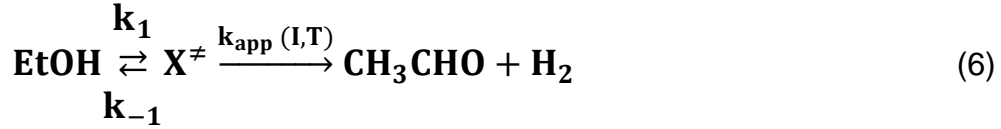
$$k_{app}(T, I) = k\,(T)I^\alpha \tag{3}$$

$$k_{app} = A\, e^{\frac{-E_a}{RT}} \tag{4}$$

where A is the pre-exponential factor, E_a is the activation energy, R is the universal gas constant and T is the absolute temperature. Eq. (4) can be written in a non-exponential form:

$$\ln k_{app} = \ln A - \frac{E_a}{RT} \tag{5}$$

The dependence of the apparent kinetic constant k_{app} on temperature can be modelled adequately with classical transition state theory (TST) [24], assuming the existence of an activated complex $X^{\neq}$ in equilibrium with the reactant

(EtOH). This assumption is consistent to previously reported details of basic mechanism of the photoreaction of EtOH on Au/TiO$_2$ [7], where an EtOH molecule is dissociatively adsorbed on the photocatalyst surface to form an ethoxide in equilibrium with the reactant, which has been the only detectable intermediate species [6]:

$$\textbf{EtOH} \underset{\textbf{k}_{-1}}{\overset{\textbf{k}_1}{\rightleftarrows}} \textbf{X}^{\neq} \xrightarrow{\textbf{k}_{app}\ \textbf{(I,T)}} \textbf{CH}_3\textbf{CHO} + \textbf{H}_2 \tag{6}$$

According to the foregoing, the equilibrium constant may be written as:

$$\textbf{K}^{\neq} = \frac{[\textbf{X}^{\neq}]}{[\textbf{EtOH}]} \tag{7}$$

and the rate for the photocatalytic hydrogen production may be expressed as follows:

$$\textbf{R}_{\textbf{H}_2} = \kappa\textbf{v}[\textbf{X}^{\neq}] \tag{8}$$

where $\textbf{v}$ is the frequency vibration, and κ is the transmission coefficient, which can be assumed equal to 1 [24]. The value of $\textbf{v}$ depends on temperature and it is independent of the nature of the reactants; therefore, once the transition state is formed, the products originate with a frequency equal to:

$$\textbf{v} = \frac{\kappa_\textbf{B}\textbf{T}}{\textbf{h}} \tag{9}$$

being $\kappa_\textbf{B}$ and $\textbf{h}$ the Boltzmann and Planck constants, respectively. Finally, substituting $[\textbf{X}^{\neq}]$ from Eq. (7) and $\textbf{v}$ from Eq. (9) into Eq. (8) we obtain:

$$\textbf{R}_{\textbf{H}_2} = \frac{\kappa_\textbf{B}\textbf{T}}{\textbf{h}}\textbf{K}^{\neq}[\textbf{EtOH}] \tag{10}$$

and the TST intrinsic kinetic rate constant $\textbf{k}$ can be expressed as:

$$\textbf{k} = \frac{\kappa_\textbf{B}\textbf{T}}{\textbf{h}}\textbf{K}^{\neq} \tag{11}$$

Taking into account the influence of the irradiance on the photocatalytic hydrogen generation an apparent kinetic constant k_{app} can be obtained:

$$k_{app}(T, I) = \frac{\kappa_B T}{h} K^{\neq} I^{\propto} \tag{12}$$

The thermodynamic parameters $\Delta G^{\neq}$, $\Delta H^{\neq}$, $\Delta S^{\neq}$ can also be calculated. For instance, it is known that the equilibrium constant $K^{\neq}$ is related to the Gibbs energy of activation, $\Delta G^{\neq}$, hence:

$$K^{\neq} = e^{\frac{-\Delta G^{\neq}}{RT}} \tag{13}$$

$$k = \frac{\kappa_B T}{h} e^{\frac{-\Delta G^{\neq}}{RT}} \tag{14}$$

Taking into account that $\Delta G^{\neq}$ depends on $\Delta H^{\neq}$ and $T\Delta S^{\neq}$:

$$\Delta G^{\neq} = \Delta H^{\neq} - T\Delta S^{\neq} \tag{15}$$

Eq (14) can be written as:

$$k = \frac{\kappa_B T}{h} e^{\frac{-(\Delta H^{\neq} - T\Delta S^{\neq})}{RT}} \tag{16}$$

By developing Eq (16) in logarithmic form at two different temperatures (T_1=298 K and T_2>T_1):

$$\ln k_1 = \ln \frac{\kappa_B T_1}{h} + \frac{\Delta S^{\neq}}{R} - \frac{\Delta H^{\neq}}{RT_1} \tag{17}$$

$$\ln k_2 = \ln \frac{\kappa_B T_2}{h} + \frac{\Delta S^{\neq}}{R} - \frac{\Delta H^{\neq}}{RT_2} \tag{18}$$

and dividing Eq. (18) by Eq (17) we obtain:

$$k_2(T_2) = k_1(T_1) \left[\frac{T_2}{T_1} e^{\frac{-\Delta H^{\neq}}{R}\left(\frac{1}{T_2} - \frac{1}{T_1}\right)} \right] \tag{19}$$

where the intrinsic kinetic rate constant k_1 at $T_1=298$ K is equal to 2.8 μmol H_2 $cm^{1.3}min^{-1} g_{cat}^{-1} mW^{-0.65}$ [21]. Now, the apparent kinetic constant k_{app} in Eq (3) can be written as:

$$k_{app}(T,I) = k_2(T_2)I^{\propto} = k_1(T_1)\left[\frac{T_2}{T_1}e^{\frac{-\Delta H^{\neq}}{R}\left(\frac{1}{T_2}-\frac{1}{T_1}\right)}\right]I^{\propto} \quad (20)$$

Finally, substituting k_{app} from Eq (20) into Eq (1) provides the rate of hydrogen production (R_{H2}), expressed in Eq (21):

$$R_{H_2} = \frac{k_1(T_1)\left[\frac{T_2}{T_1}e^{\frac{-\Delta H^{\neq}}{R}\left(\frac{1}{T_2}-\frac{1}{T_1}\right)}\right]I^{\propto} KP_{EtOH}}{1+KP_{EtOH}} \quad (21)$$

The generation of hydrogen obtained experimentally at different temperatures and irradiances was fitted to the kinetic model described in Eq. (21) by means of nonlinear generalized reduced gradient (GRG). This algorithm allowed minimizing the objective function for normalized residual sum of squares (NRSS):

$$NRSS = \sum_{n=1}^{N}\left(\frac{R_{e,n}-R_n}{R_n}\right)^2 \quad (22)$$

where $R_{e,n}$ is the reaction rate estimated by the model, R_n corresponds to the n value of the experimental hydrogen production rate, and N is the total number of experiments. Finally, the entropy of activation can be calculated using Eq. (23)

$$\Delta S^{\neq} = \frac{(\Delta H^{\neq}-\Delta G^{\neq})}{T} \quad (23)$$

4. Results and discussion

4.1. Hydrogen production as function of temperature and UVA irradiation

The effect of temperature and different light intensities was investigated at 298, 323 and 348 K for indoor photocatalytic tests. The kinetic analysis was conducted under differential conditions, at ethanol conversions well below 5%, and the results are summarized in Fig.3. In all cases, steady state was rapidly achieved.
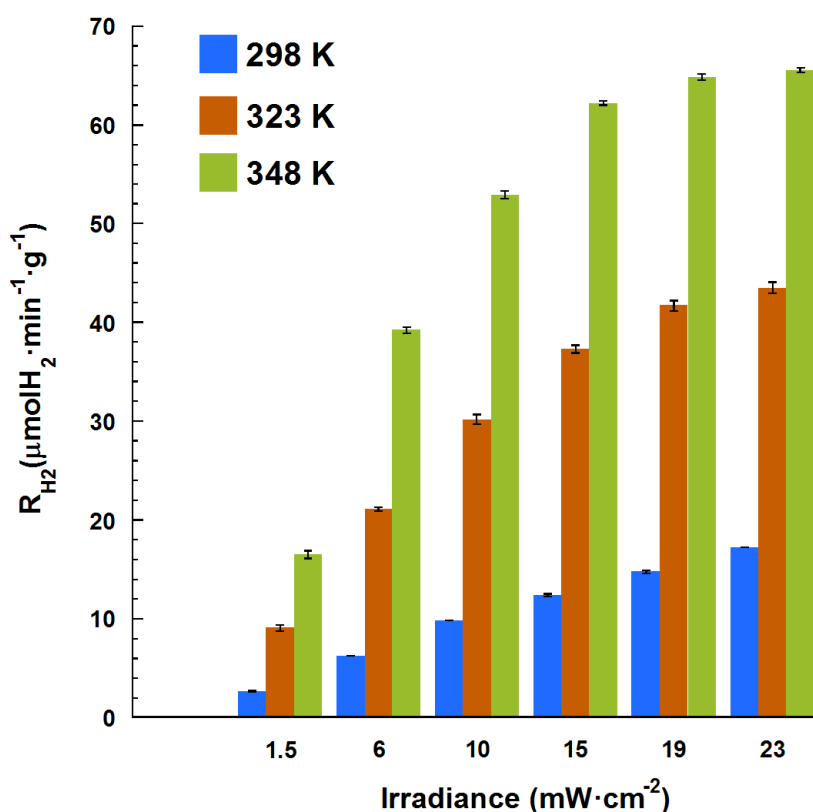

Figure 3. Hydrogen photoproduction rates obtained at different temperatures under different UVA light intensity values (residence time 0.35 s, GHSV=10,200 h^{-1}, H_2O:EtOH=9:1 molar). The error bars correspond to the standard deviation of four measurements.

Photocatalytic hydrogen generation is always favored by increasing the temperature within the range used. Also, hydrogen production rates for a given temperature increase with light intensity. However, whereas they increase practically linear at 298 K, at higher temperatures the generation of hydrogen only increase linearly up to ca. 10 mW·cm^{-2}, and at higher light intensity values the hydrogen photoproduction rates increase slowly. Therefore it is clear that, for a given light intensity, H$_2$ photoproduction increases strongly with temperature. At 298 K (room temperature) and 1.5 mW·cm^{-2} the amount of H$_2$ produced is 2.7±0.1 μmol·min^{-1}·g^{-1}, whereas at 323 K the amount of H$_2$ increases up to 9.1±0.3 μmol·min^{-1}·g^{-1} under the same irradiance (~3.4 enhancement factor). By further elevating the temperature up to 348 K the hydrogen production rate is remarkably higher, 16.5±0.4 μmol·min^{-1}·g^{-1}, which represents an enhancement factor of about 6 with respect to the value obtained at room temperature. Actually, it is well known that adsorption energies of acetaldehyde on inorganic oxides are higher than adsorption energies of ethanol and, as a result, the blockage of active sites of the catalysts takes place [25]. For that reason, the beneficial effect of temperature could be due to a weaker adsorption of acetaldehyde on the photocatalytic surface, resulting in the unblocking of the active sites of the catalyst, in accordance with a previous work [10]. However, it should be stressed out that the enhancement of the hydrogen photoproduction rate is not directly proportional to the temperature value in the range studied. In particular, the enhancement factor is progressively lower when the temperature is increased. This may indicate that, the higher the temperature the higher the electron-hole recombination rate. In fact, previous works reported temperature-dependent charge carrier mobility.

For instance, Kim *et al.* estimated for a single-crystalline TiO_2 that increasing the reaction temperature from 298 K to 353 K the hole mobility was increased by two orders of magnitude [17]. Kopidakis *et al.* experimentally observed a temperature dependence of the electron diffusion coefficient, improving ca. 10 times the diffusion coefficients with increasing temperatures from 298 to 348K [26]. Hagfeldt and coworkers studied the temperature dependence of the charge transport in nanostructured TiO_2 films, demonstrating an increase of conductivity with increasing temperature [27]. Therefore, the effect of temperature likely has a double effect, on one hand it favors the photogeneration of hydrogen by favoring the desorption of acetaldehyde produced during the photoreaction but, on the other hand, accelerates the electron-hole recombination rate. Consequently, the optimum temperature for the photogeneration of hydrogen may depend not only on the electron sequestration capacity of the titania modified with metal nanoparticles, but also on the hole scavenger agent used and, in particular, on the adsorption strength of the oxidation products generated by the reaction between the sacrificial agent and the holes in the valence band.

For further evaluation of the process the apparent quantum efficiency (AQE) was calculated for each temperature at 1.5 mW·cm^{-2} by using the equation AQE=$(2 \cdot R_{H2}/N_\lambda) \cdot 100$ [18,28] being the overall amount of photons reaching the microreactor, N_λ, equal to 0.58 µmol photons·min^{-1} [20]. This light intensity value has been selected taking into account the linear relationship between the hydrogen production rate and light irradiance in the range 1.5-10 mW·cm^{-2} for all temperatures tested (no photon transfer limitations). The efficiency of light to-

hydrogen (LTH) energy conversion, defined as the energy stored as hydrogen ($R_{H2} \cdot \Delta H_{c,H2}$, where $\Delta H_{c,H2}$ is the higher heating value of hydrogen, 285.8 kJ·mol^{-1}) divided by the total incident photon power over the irradiated area of ca. 2.12 cm^2 (3.17 mW) was also calculated [18,20]. The values are reported in Table 1. Clearly, the positive effect of temperature is observed over both the AQE and LTH values.

Table 1. Apparent quantum efficiency (AQE) and light to hydrogen (LTH) conversion efficiency obtained at 1.5 mW·cm^{-2} UVA and 0.005 g of Au/TiO$_2$ photocatalyst.

T (K)	R_{H2} (µmol·min^{-1})	AQE (%)	LTH (%)
298	0.013	4.6	2
323	0.046	15.7	6.8
348	0.083	28.4	12.4

The activation energy for the photogeneration of H$_2$ can be calculated following the Arrhenius equation (Eq. 5). Fig. 4 shows a linear dependence of ln k_{app} versus 1/T for light irradiances of 1.5 to 15 mW·cm^{-2}. As expected, parallel straight lines are obtained, which define an activation energy of 24±1 kJ·mol^{-1}. This value is in accordance with those reported by other authors for the same reaction over Au/TiO$_2$ photocatalyst, 30.3 kJ·mol^{-1} [10], or for Pd/TiO$_2$ systems, 10-25 kJ·mol^{-1} [5,17].
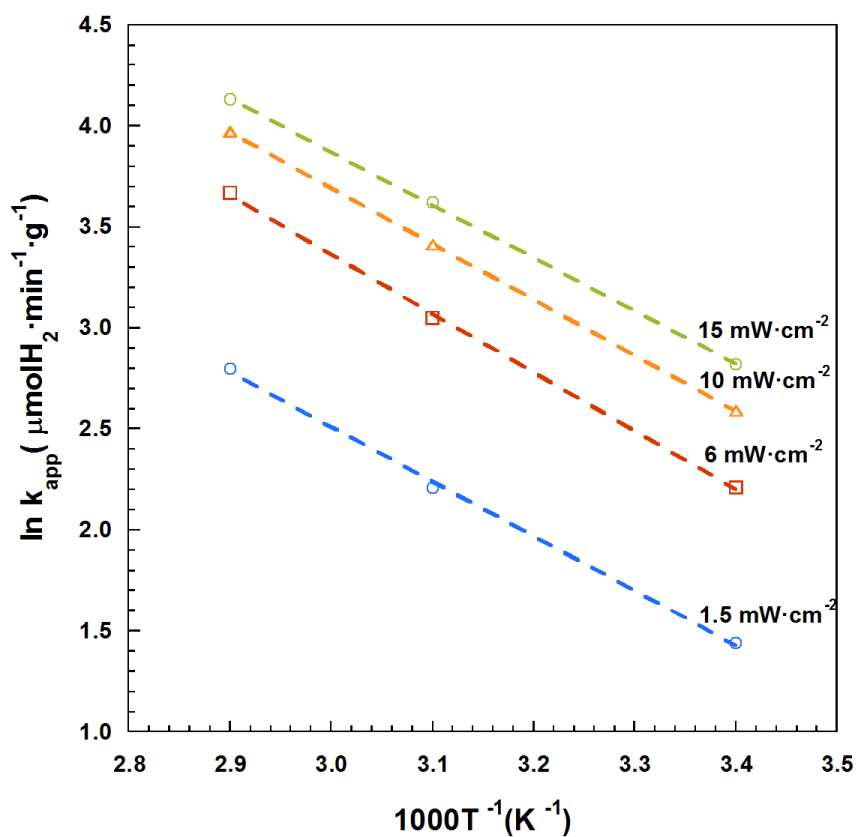
Figure 4. Arrhenius plots corresponding to the experiments conducted at 1.5 to 15 mW·cm^{-2} UVA at 298-348 K.

The hydrogen photoproduction rates at different temperature and irradiance values are well described by Eq. (21). The parity plot in Fig. 5 shows a very good correlation between the model and the experimental data. The best fit was obtained for a $\Delta H^{\neq}$ value of about 27.5 kJ·mol^{-1}, with an NRSS value of 0.26.
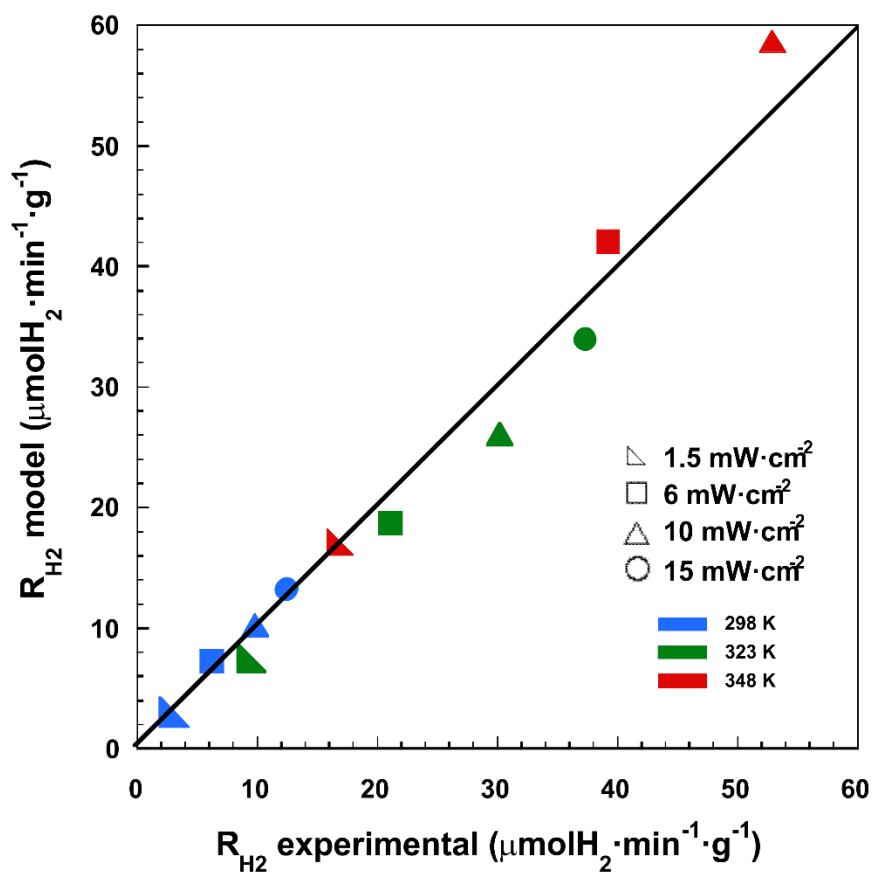
Figure 5 Parity plot of the experimental hydrogen photoproduction rates obtained at GHSV=10,200 h^{-1} for different light intensity values and temperatures (298, 323 and 348 K) against the model results calculated from Eq. (21).

The equilibrium constant $\mathbf{K}^{\neq}$, Gibbs free energy activation, $\Delta\mathbf{G}^{\neq}$, and entropy of activation, $\Delta\mathbf{S}^{\neq}$, were calculated at each temperature using; Eq. 11, Eq. 13 and Eq. 23, respectively. Kinetic and thermodynamic parameters are summarized in Table 2.

Table 2. Kinetic and thermodynamic parameters for the photocatalytic H_2 production over Au/TiO$_2$.

T (K)	k (T) (μmol H$_2$·cm$^{1.3}$·min^{-1}·g^{-1}·mW$^{-0.65}$)	K$^{\neq}$(T) (μmol H$_2$·cm$^{1.3}$·g^{-1}·mW$^{-0.65}$)	ΔG$^{\neq}$ (kJ·mol^{-1})	ΔH$^{\neq}$ (kJ·mol^{-1})	ΔS$^{\neq}$ (kJ·K^{-1}·mol^{-1})
298	2.8	7.4x10^{-15}	80.7	27.5	-0.182
323	6.7	1.7x10^{-14}	85.2		
348	14.7	3.4x10^{-14}	89.7		

The positive value of $\Delta H^{\neq}$ and the progressively increasing value of the intrinsic kinetic rate constant **k** with temperature indicate that the H$_2$ photoproduction from water-ethanol using Au/TiO$_2$ is an endothermic process. Also, the increasing value of $\Delta G^{\neq}$ with temperature indicates the non-spontaneous nature of the process. The negative value of $\Delta S^{\neq}$ is commonly observed and it is ascribed to the change in the configuration of the reactant species along the reaction path, where the formation of the activated complex involves the loss of freedom degrees [24].

Therefore, our findings are consistent with the photocatalytic cycle involved in the photo-production of hydrogen from EtOH over Au/TiO$_2$ previously proposed by Idriss and coworkers [6,7]. Briefly, an EtOH molecule is dissociatively adsorbed on the photocatalyst surface to form an ethoxide in equilibrium with the reactant, as we stated in Eq. (6), and a hydrogen ion (as a surface hydroxyl). Then, ethoxides inject two electrons into the valence band and acetaldehyde is produced, and two hydrogen ions are reduced to a hydrogen molecule by two electrons from the conduction band. The presence of water is important to avoid the blockage of the active sites of the photocatalyst by

adsorption of acetaldehyde molecules. In our case of study, water molecules do not participate in the kinetic modelling because the partial pressure of water was much higher than the partial pressure of ethanol thus leading to a pseudo first-order kinetics on the limiting reactant, i.e., ethanol.

4.2. Hydrogen production outdoor by using a solar concentrator

The outdoor experiments were carried out aimed at evaluating both the hydrogen photoproduction process under real conditions up to 423 K (direct concentrated sunlight, Fig. 2) and the scale up of the microreactor concept. As explained in the experimental section, two different microreactors were tested, being one of them the result of scaling up by one order of magnitude (Fig. 1). As expected from the study reported in section 4.1, an increase of temperature resulted in higher photoactivity (Fig. 6), thus confirming that temperature (from the solar concentrator) has a positive effect in the photogeneration of hydrogen. The activation energy determined from the Arrhenius equation Eq. (5) was ~26 $kJ \cdot mol^{-1}$ (see inset in Fig. 6), in accordance with the results obtained in the indoor experiments reported above. It should be noted that the control of the temperature in the outdoor experiments was more difficult to achieve than in the indoor case. The experimental conditions for outdoor experiments were intrinsically dynamic due to Earth's orbit, length of the exposition to solar radiation and weather conditions, which caused oscillations during the measurements of temperature with a standard error of ±5 K. Similarly, the measurement of the UVA radiation yielded values in the range 40-60 $mW \cdot cm^{-2}$. It was observed that the hydrogen photoproduction rates obtained in the indoor

(Fig. 3) and outdoor (Fig. 6) experiments at 323 and 348 K were similar. However, the outdoor experiments carried out with the solar concentrator at higher temperatures (up to 423 K, which was the stability limit of the silicone microreactors) yielded remarkable hydrogen photoproduction rates. In contrast to the indoor experiments carried out with solely UVA radiation, the use of concentrated sunlight proved to be effective in spanning the operational temperature range. This might be due not only to a positive effect of temperature, but also to the intrinsic wavelength distribution of the solar spectrum.
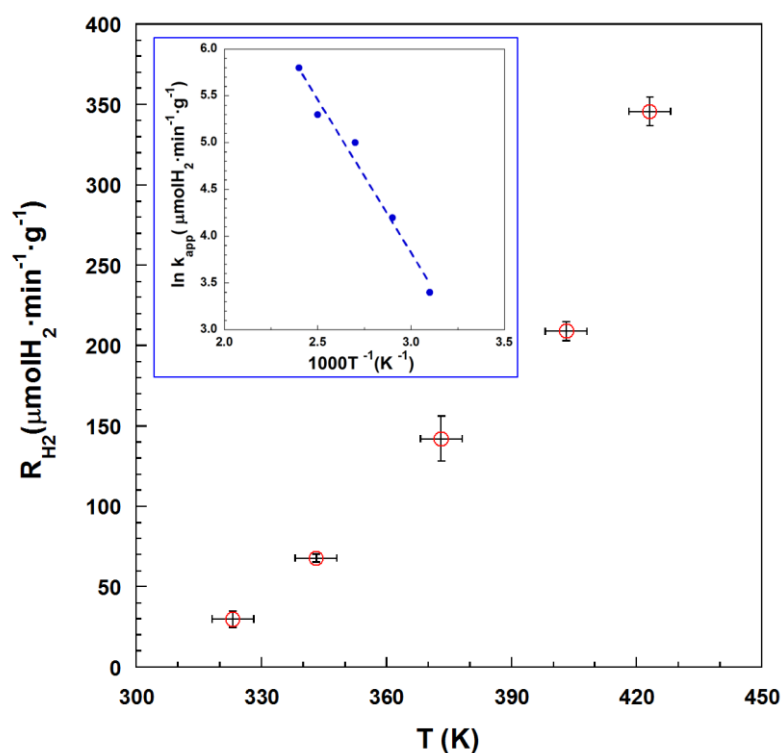

Figure 6. Photocatalytic hydrogen generation rates obtained at different temperatures under sunlight irradiance (residence time 0.35 s, GHSV=10,200 h^{-1}, H_2O:EtOH=9:1 molar). The error bars correspond to the standard deviation of four measurements.

Finally, the study of the scale up of the process was carried out at 323-373 K by using the two microreactors depicted in Fig. 1. Fig. 7 shows a parity plot with the hydrogen photoproduction rates obtained over both microreactors normalized per irradiated area of catalyst. A good correspondence between the data obtained over the two microreactors is observed, which demonstrates that direct scaling up is feasible.
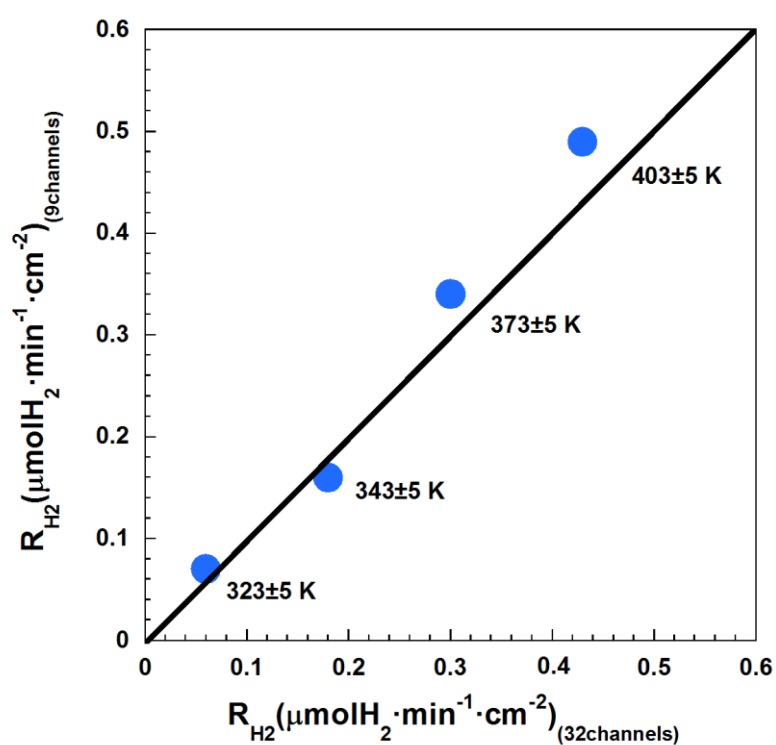

Figure 7. Hydrogen photoproduction rates normalized per irradiated area of catalyst obtained over the two silicone microreactors shown in Fig. 1.

5. Conclusions

The effect of temperature on the gas-phase photocatalytic H_2 production from a water:ethanol mixture has been studied using silicone microreactors loaded with

Au/TiO$_2$ photocatalyst under UVA and sunlight irradiance. An increase of temperature favors the generation of hydrogen at different irradiances following the Arrhenius relation. The activation energy of the photocatalytic process has been found to be 24±1 kJ·mol^{-1}. The generation of hydrogen obtained experimentally at different temperatures and irradiances has been fitted to a kinetic model taking into account the transition state theory. It has been encountered that, under UVA radiation, temperature has a double effect; on one hand it enhances the H$_2$ photoproduction by possibly favoring the desorption of acetaldehyde but, on the other hand, it also favors electron-hole recombination. Additionally, we have demonstrated an easy and cheap scale up using silicone microreactors and a solar concentrator. The experimental results and the kinetic model reported here is of importance for the design of new and more efficient photo-microreactors for solar driven hydrogen production.

Acknowledgments

References

[1]   Dincer I, Acar C. Review and evaluation of hydrogen production methods

for better sustainability. Int J Hydrogen Energy 2014;40:11094–111.

[2]   Gandía LM, Arzamendi G, Diéguez PM. Renewable Hydrogen Energy: An
        Overview. In: Gandía LM, Arzamendi G, Diéguez PM, editors. Renew.
        Hydrog. Technol. Prod. Purification, Storage, Appl. Saf., Oxford, UK:
        2013, p. 1–17.

[3]   Yerga RMN, Alvarez-Galván MC, Vaquero F, Arenales J, Fierro JLG.
        Hydrogen Production from Water Splitting Using Photo-Semiconductor
        Catalyst. In: Gandía LM, Arzamendi G, Diéguez PM, editors. Renew.
        Hydrog. Technol. Prod. Purification, Storage, Appl. Saf., Oxford, UK:
        2013, p. 43–59.

[4]   Bamwenda GR, Tsubota S, Nakamura T, Haruta M. Photoassisted
        hydrogen production from a water-ethanol solution: a comparison of
        activities of AuTiO2 and PtTiO2. J Photochem Photobiol A Chem
        1995;89:177–89.

[5]   Yang YZ, Chang C-H, Idriss H. Photo-catalytic production of hydrogen
        form ethanol over M/TiO2 catalysts (M = Pd, Pt or Rh). Appl Catal B
        Environ 2006;67:217–22.

[6]   Nadeem MA, Murdoch M, Waterhouse GIN, Metson JB, Keane MA,
        Llorca J, et al. Photoreaction of ethanol on Au/TiO2 anatase: Comparing
        the micro to nanoparticle size activities of the support for hydrogen
        production. J Photochem Photobiol A Chem 2010;216:250–5.

[7]   Murdoch M, Waterhouse GIN, Nadeem MA, Metson JB, Keane MA, Howe
        RF, et al. The effect of gold loading and particle size on photocatalytic
        hydrogen production from ethanol over Au/TiO$_2$ nanoparticles. Nat Chem
        2011;3:489–92.

[8]   Connelly K, Wahab AK, Idriss H. Photoreaction of Au/TiO2 for hydrogen production from renewables: a review on the synergistic effect between anatase and rutile phases of TiO2. Mater Renew Sustain Energy 2012;1:3.

[9]   Jovic V, Chen WT, Sun-Waterhouse D, Blackford MG, Idriss H, Waterhouse GIN. Effect of gold loading and TiO2 support composition on the activity of Au/TiO2 photocatalysts for H2 production from ethanol-water mixtures. J Catal 2013;305:307–17.

[10]   Taboada E, Angurell I, Llorca J. Dynamic photocatalytic hydrogen production from ethanol–water mixtures in an optical fiber honeycomb reactor loaded with Au/TiO2. J Catal 2014;309:460–7.

[11]   Bonmatí E, Casanovas A, Angurell I, Llorca J. Hydrogen Photoproduction from Ethanol-Water Mixtures over Au-Cu Alloy Nanoparticles Supported on TiO2. Top Catal 2015;58:77–84.

[12]   Shimura K, Yoshida H. Heterogeneous photocatalytic hydrogen production from water and biomass derivatives. Energy Environ Sci 2011;4:2467–81.

[13]   Llorca J, Corberán VC, Divins NJ, Olivera Fraile R, Taboada E. Hydrogen from Bioethanol. In: Gandía LM, Arzamendi G, Diéguez PM, editors. Renew. Hydrog. Technol. Prod. Purification, Storage, Appl. Saf., Oxford, UK: 2013, p. 135–70.

[14]   Taboada E, Angurell I, Llorca J. Hydrogen photoproduction from bio-derived alcohols in an optical fiber honeycomb reactor loaded with Au/TiO2. J Photochem Photobiol A Chem 2014;281:35–9.

[15]   Nomikos GN, Panagiotopoulou P, Kondarides DI, Verykios XE. Kinetic

and mechanistic study of the photocatalytic reforming of methanol over Pt/TiO2 catalyst. Appl Catal B Environ 2014;146:249–57.

[16] Bell S, Will G, Bell J. Light intensity effects on photocatalytic water splitting with a titania catalyst. Int J Hydrogen Energy 2013;38:6938–47.

[17] Kim G, Choi HJ, Kim H, Kim J, Monllor-Satoca D, Kim M, et al. Temperature-boosted photocatalytic H2 production and charge transfer kinetics on TiO2 under UV and visible light. Photochem Photobiol Sci 2016;15:1247–53.

[18] Ye L, Chu KH, Wang B, Wu D, Xie H, Huang G, et al. Noble-metal loading reverses the temperature dependent photocatalytic hydrogen generation in methanol-water solution. Chem Commun 2016;52:11657–60.

[19] Primo A, García H. Solar Photocatalysis for Environment Remediation. In: Suib SL, editor. New Futur. Dev. Catal. Sol. Photocatal., Oxford, UK: 2013, p. 145–65.

[20] Castedo A, Mendoza E, Angurell I, Llorca J. Silicone microreactors for the photocatalytic generation of hydrogen. Catal Today 2016;273:106–11.

[21] Castedo A, Uriz I, Soler L, Gandía LMLM, Llorca J. Kinetic analysis and CFD simulations of the photocatalytic production of hydrogen in silicone microreactors from water-ethanol mixtures. Appl Catal B Environ 2017;203:210–7.

[22] Brust M, Walker M, Bethell D, Schiffrin DJ, Whyman R. Synthesis of Thiol-derivatised Gold Nanoparticles in Two-phase Liquid-Liquid System. J Chem Soc, Chem Commun 1994:801–2.

[23] Llorca J, Domínguez M, Ledesma C, Chimentao R, Medina F, Sueiras J, et al. Propene epoxidation over TiO2-supported Au–Cu alloy catalysts

prepared from thiol-capped nanoparticles. J Catal 2008;258:187–98.

[24] Schaleger LL, Long FA. Entropies of Activation and Mechanisms of Reactions in Solution. Adv Phys Org Chem 1963;1:1–33.

[25] Guil JM, Homs N, Llorca J, De La Piscina PR. Microcalorimetric and infrared studies of ethanol and acetaldehyde adsorption to investigate the ethanol steam reforming on supported cobalt catalysts. J Phys Chem B 2005;109:10813–9.

[26] Kopidakis N, Benkstein KD, Van De Lagemaat J, Frank AJ, Yuan Q, Schiff EA. Temperature dependence of the electron diffusion coefficient in electrolyte-filled TiO2 nanoparticle films: Evidence against multiple trapping in exponential conduction-band tails. Phys Rev B - Condens Matter Mater Phys 2006;73:45326.

[27] Agrell HG, Boschloo G, Hagfeldt A. Conductivity studies of nanostructured TiO2 films permeated with electrolyte. J Phys Chem B 2004;108:12388–96.

[28] Yu Y-G, Chen G, Hao L-X, Zhou Y-S, Wang Y, Pei J, et al. Doping La into the depletion layer of the Cd0.6Zn0.4S photocatalyst for efficient H2 evolution. Chem Commun 2013;49:10142.